

Reconstructors for Fourier-based wavefront sensors derived from mathematical models

Victoria Hutterer

Industrial Mathematics Institute, Johannes Kepler University, Linz, Austria.

Joint work with: Iuliia Shatkhina, Olivier Fauvarque, Andreas Obereder, Pierre Janin-Potiron, Stefan Raffetseder, Vincent Chambouleyron, Yoann Brûlé, Ronny Ramlau, Benoit Neichel, Thierry Fusco, Carlos Correia.



**SFB Tomography
Across the Scales**

LAM Marseille, February 28, 2019

Outline:

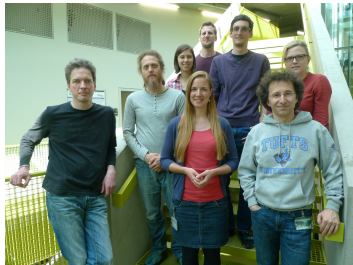
- Fourier-based wavefront sensors in astronomical Adaptive Optics
- Underlying mathematical models
- Model-based wavefront reconstruction methods



Credit: NASA

ELT - the world's biggest eye on the sky

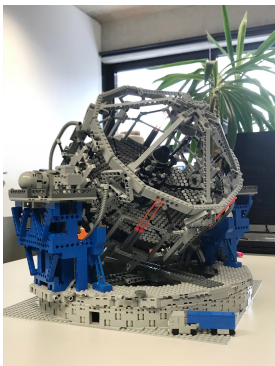
- Austrian scientific contribution:
"Mathematical algorithms and software for ELT adaptive optics"
- Austrian Adaptive Optics (AAO) team in Linz
- ELT instruments METIS & MICADO



Credit: ESO

Austrian Adaptive Optics

working on:



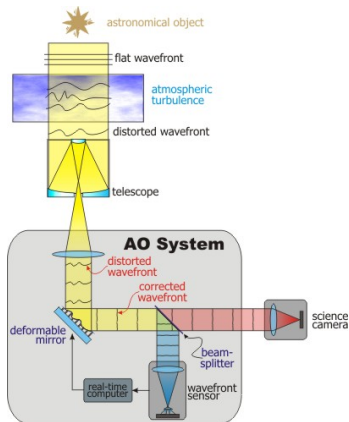
- wavefront reconstruction for ELTs
- Shack-Hartmann and pyramid WFS
- atmospheric tomography
- PSF reconstruction
- optimal control
- ...



<https://www.facebook.com/TomographyAcrossTheScales/>

Adaptive Optics (AO)

Adaptive Optics is a technique for correcting optical distortions arising during the imaging process ~ hardware based real-time deblurring



Credit: C. Max

components of AO system:

- deformable mirrors
- wavefront sensors
- control system
→ inverse problem

Inverse problem of wavefront reconstruction

Wavefront sensors (WFSs) provide intensity measurements which are related in a (non-linear) way to the wavefront of the incoming light.

$$\mathbf{s} = \mathbf{W}\phi + \eta.$$

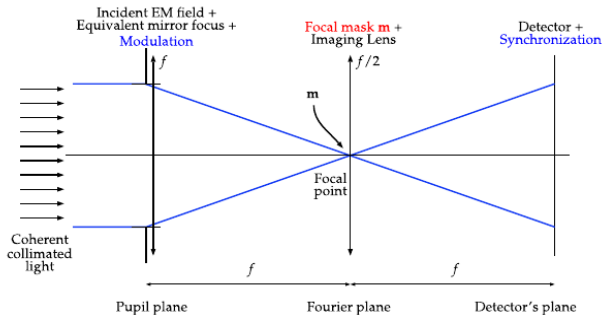
Diagram illustrating the wavefront reconstruction equation:

- \mathbf{W} : WFS operator
- ϕ : incoming phase
- η : unpredictable noise
- \mathbf{s} : WFS measurements

Arrows indicate the flow of information: ϕ and η contribute to \mathbf{s} via \mathbf{W} . The labels "WFS operator" and "unpredictable noise" are positioned above the equation, while "WFS measurements" and "incoming phase" are positioned below it.

Restoration of the unknown wavefront from given sensor measurements and further calculation of optimal mirror deformation is an **inverse problem**.

Fourier filtering optical system

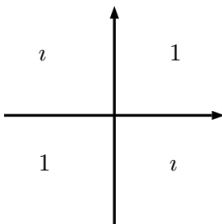


Credit: O. Fauvarque

$$I(x, y) = |\mathcal{F}^{-1} (OTF \cdot \mathcal{F} (\chi_{\Omega} e^{-i\Phi}))|^2$$

i Quad wavefront sensor: a new Fourier-based WFS

- derived from the 4-quadrants coronagraph
- focal plane is divided into 4 quadrants around the origin
- each quadrant is $\pi/2$ shifted with its 2 neighbours



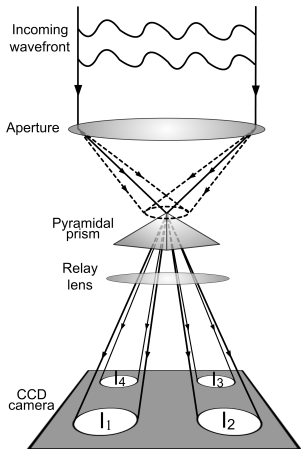
Transparency function of the 4-quadrants sensing mask

Pyramid wavefront sensor: baseline for many future ELT instruments



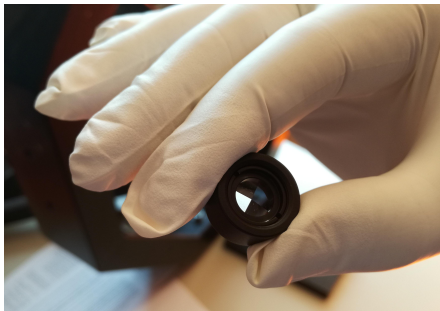
Extremely Large Telescope, Very Large Telescope, and the Pyramids of Giza, Credit: ESO

Pyramid wavefront sensor

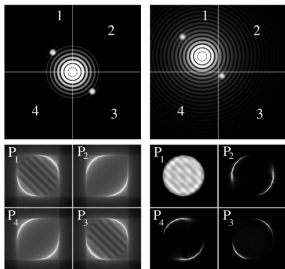


Credit: Iu. Shatokhina

- (oscillating) pyramidal prism
- splits light into 4 distinct directions
- 4 intensities are measured
- those can be combined to 2 signals



Pyramid wavefront sensor (PWFS) measurements

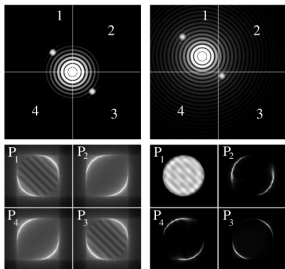


Credit: O. Guyon

modulation of the beam:

- increased linear range
- reduced sensitivity

Pyramid wavefront sensor (PWFS) measurements



Credit: O. Guyon

modulation of the beam:

- increased linear range
- reduced sensitivity

$$s_x(x, y) = \frac{[I_1(x, y) + I_2(x, y)] - [I_3(x, y) + I_4(x, y)]}{I_0}$$

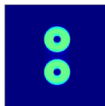
$$s_y(x, y) = \frac{[I_1(x, y) + I_4(x, y)] - [I_2(x, y) + I_3(x, y)]}{I_0}$$

I_0 – average intensity per subaperture

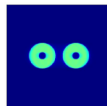
Different concepts of a pyramid sensor

different configurations of prism:

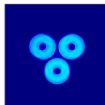
- a) 2-sided (roof) prism
- b) 2-sided (roof) prism
- c) 3-sided
- d) 4-sided
- e) 6-sided
- f) cone



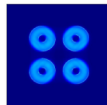
(a)



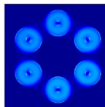
(b)



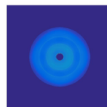
(c)



(d)



(e)



(f)

Credit: B. Engler

Problem description

Pyramid sensor measuring process:

$$P\Phi = s$$

(Φ ... incoming wavefront, s ... pyramid sensor measurements)

interaction-matrix-based:

\bar{P} ... calibrated matrix

This is the benchmark with respect to quality and speed.

model-based:

P ... non-linear operator

This is the basis of the new methods.

Outline:

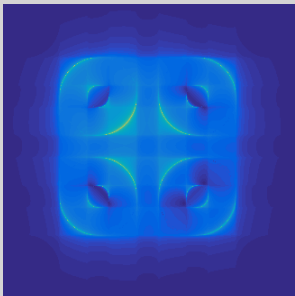
- Fourier-based wavefront sensors in astronomical Adaptive Optics
- Underlying mathematical models
- Model-based wavefront reconstruction methods



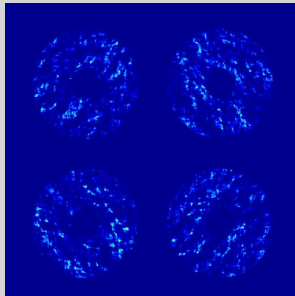
Credit: NASA

How do we model it mathematically?

phase mask model
underlying model
in forward simulations



transmission mask model
underlying model
of reconstructors



Credit: Iu. Shatokhina

PWFS transmission mask models

Theorem

The relation between pyramid wavefront sensor data **with circular modulation** and the incoming phase following the transmission mask model is given by

$$s_x^c(x, y) = \frac{1}{2\pi} \mathcal{X}_{\Omega}^c(x, y) \int_{\Omega_y} \frac{\sin[\Phi(x', y) - \Phi(x, y)] J_0[\alpha_\lambda(x' - x)]}{x - x'} dx'$$

$$+ \frac{1}{2\pi^3} \mathcal{X}_{\Omega_y}^c(x, y) \text{ p.v.} \int_{\Omega_y} \int_{\Omega_x} \int_{\Omega_x} \frac{\sin[\Phi(x', y') - \Phi(x, y'')] f(x' - x, y' - y'')}{(x - x')(y - y')(y - y'')} dy'' dy' dx',$$

$$f(\tilde{x}, \tilde{y}) := \frac{1}{T} \int_{-T/2}^{T/2} \cos[\alpha_\lambda \tilde{x} \sin(2\pi t/T)] \cos[\alpha_\lambda \tilde{y} \cos(2\pi t/T)] dt$$

and s_y accordingly.

J_0 ... zero order Bessel function of first kind

α_λ ... modulation parameter

Pyramid WFS without modulation

Theorem

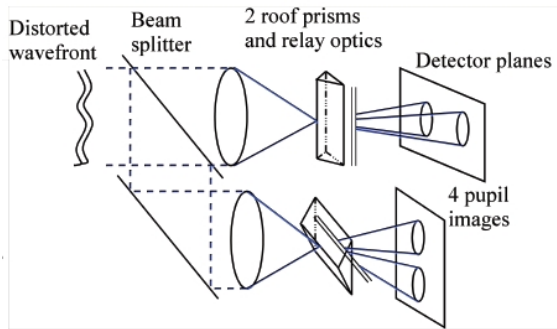
The measurements of the PWFS without modulation are given by

$$s_x(x, y) = \frac{1}{2\pi} \mathcal{X}_{\Omega} (x, y) \int_{\Omega_y} \frac{\sin[\Phi(x', y) - \Phi(x, y)]}{x - x'} dx' \\ + \frac{1}{2\pi^3} \mathcal{X}_{\Omega_y} (x, y) \text{ p.v.} \int_{\Omega_y} \int_{\Omega_x} \int_{\Omega_x} \frac{\sin[\Phi(x', y') - \Phi(x, y'')]}{(x - x')(y - y')(y - y'')} dy'' dy' dx',$$

assumptions:

- **roof wavefront sensor**

Roof WFS approximation



Credit: C. Véraud

Pyramid WFS without modulation

Theorem

The measurements of the PWFS without modulation are approximated by

$$s_x(x, y) \sim \frac{1}{2\pi} \mathcal{X}_\Omega(x, y) \int_{\Omega_y} \frac{\sin[\Phi(x', y) - \Phi(x, y)]}{x - x'} dx'$$

assumptions:

- **roof wavefront sensor**
 - substitute four-sided prism by two orthogonally placed two-sided prisms
 - two signal sets s_x and s_y are independent and contain information about Φ only in x - and only in y -direction correspondingly
- small wavefront distortions (as expected in closed loop),
 $\Phi \ll 1 \rightarrow \sin \Phi \simeq \Phi$
- without second term

Pyramid WFS without modulation

Theorem

The measurements of the PWFS without modulation are approximated by

$$s_x(x, y) \sim \frac{1}{2\pi} \mathcal{K}_\Omega(x, y) \int_{\Omega_y} \frac{\sin[\Phi(x', y) - \Phi(x, y)]}{x - x'} dx'$$

assumptions:

- **roof wavefront sensor**
 - substitute four-sided prism by two orthogonally placed two-sided prisms
 - two signal sets s_x and s_y are independent and contain information about Φ only in x - and only in y -direction correspondingly
- small wavefront distortions (as expected in closed loop),
 $\Phi \ll 1 \rightarrow \sin \Phi \simeq \Phi$
- without second term

Pyramid WFS without modulation

Theorem

The measurements of the PWFS without modulation are approximated by

$$s_x(x, y) \sim \frac{1}{2\pi} \mathcal{X}_\Omega(x, y) \int_{\Omega_y} \frac{\sin[\Phi(x', y) - \Phi(x, y)]}{x - x'} dx'$$

assumptions:

- **roof wavefront sensor**
 - substitute four-sided prism by two orthogonally placed two-sided prisms
 - two signal sets s_x and s_y are independent and contain information about Φ only in x - and only in y -direction correspondingly
- small wavefront distortions (as expected in closed loop),
 $\Phi \ll 1 \rightarrow \sin \Phi \simeq \Phi$
- without second term

Outline:

- Fourier-based wavefront sensors in astronomical Adaptive Optics
- Underlying mathematical models
- Model-based wavefront reconstruction methods



Credit: NASA

Preprocessed CuReD (P-CuReD)

assumption: closed loop AO.

$$\text{P-CuReD} = \text{data preprocessing} + \text{CuReD}$$

two-step method:

- **data preprocessing:** transform the PWFS data to SH-like data according to the analytical relation in the Fourier domain.
- **CuReD:** apply the CuReD to the modified data.
(CuReD is a very efficient reconstructor for SH WFS, linear complexity)

Step 1: data preprocessing [Iu. Shatokhina]

representation of the measurements in the Fourier domain

$$(\mathcal{F}S_{pyr})(u) = (\mathcal{F}\Phi)(u) \cdot g_{pyr}(u) \cdot \text{sinc}(du)$$

$$(\mathcal{F}S_{sh})(u) = (\mathcal{F}\Phi)(u) \cdot g_{sh}(u) \cdot \text{sinc}(du)$$

u – spatial frequency, d – subaperture size.

Fourier domain relation between the two sensors

$$(\mathcal{F}S_{sh})(u) = (\mathcal{F}S_{pyr})(u) \cdot g_{sh/pyr}(u), \quad g_{sh/pyr}(u) := \frac{g_{sh}(u)}{g_{pyr}(u)}.$$

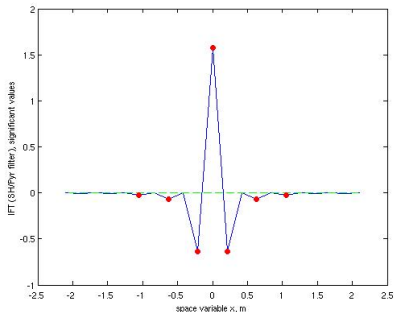
Fourier convolution theorem → relation between the two sensors in the space domain

$$s_{sh}(x, y) = \frac{1}{\sqrt{2\pi}} s_{pyr}(\cdot, y) * \underbrace{(\mathcal{F}^{-1} g_{sh/pyr})(\cdot)}_{p_{sh/pyr}(x)}.$$

Step 1: data preprocessing [Iu. Shatokhina]

convolve data set with 1d kernel $p_{sh/pyr}$

$$S_{sh}(x, y) = \frac{1}{\sqrt{2\pi}} S_{pyr}(\cdot, y) * p_{sh/pyr}(\cdot).$$



computationally very cheap, highly parallelizable and pipelinable

Step 2: application of CuReD [M. Rosensteiner]

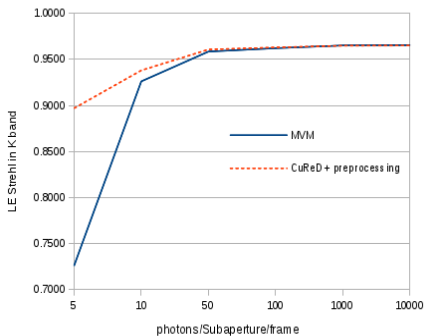
28./29. September 2012: CuReD on sky, Herschel telescope

- Las Palmas, Canary Islands (Spain), Roque de los Muchachos (2344m)
- 4.2 m mirror diameter
- successful CuReD-tests of the University of Durham, code from AAO team

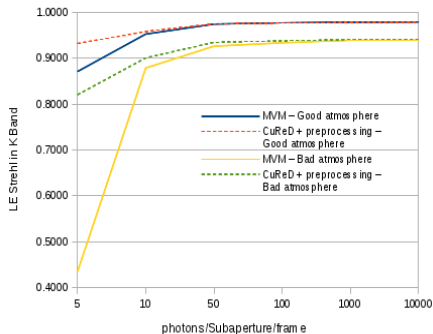


Quality and speed performance

LE Strehl in K band: MVM and P-CuReD vs. the detected NGS photon flux.



ESO median atmosphere



ESO bad/good atmospheres

P-CuReD on the LOOPS bench

- application of a model-based reconstructor on LOOPS
- closed the loop for both PWFS with & without modulation
- reconstruction quality comparable to approach with calibrated MVM

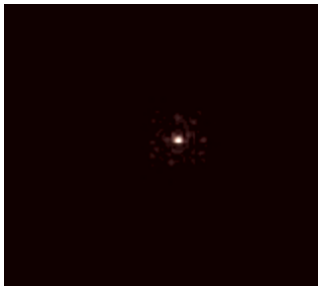


Figure: closing the loop on LOOPS with P-CuReD

Recent ELT adaptations: telescope spiders

- pupil fragmentation & **disconnectedness of data** (wavefront information)
- differential piston effects between the segments
- if not properly handled extremely poor wavefront reconstruction

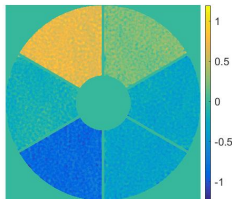


Figure: residual phase in radians (K-band)

How much quality do we lose in the presence of spiders?
How can we make existing reconstruction methods feasible?

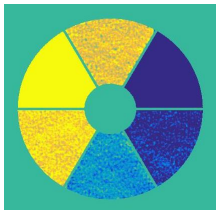
Split Approach

Split Approach =

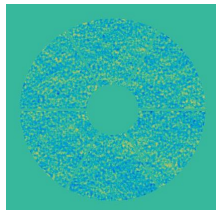
piston-free WF reconstruction + direct segment piston reconstruction

Requests:

- compoundable with all existing reconstruction methods
- providing high reconstruction quality
- low computational complexity



Split Approach →



Quad wavefront sensor: first numerical results - "optical" linear Landweber iteration

minimize least-squares functional

$$J(\Phi) := \|ml(\Phi_\gamma) - Q(\Phi_\gamma)\|_{\mathcal{L}_2}^2 \quad \rightarrow \quad \min$$
$$J'(\Phi) = Q^*(Q\Phi_\gamma - ml(\Phi_\gamma))$$

linear iterative Landweber algorithm:

$$\Phi_{k+1} = \Phi_k + \alpha Q^*(ml(\Phi_\gamma) - Q(\Phi_k))$$

Φ_γ is the phase-to-be-measured/reconstructed, Q the wavefront sensor operator and $ml(\Phi_\gamma)$ the corresponding meta-intensity.

Quad wavefront sensor: first numerical results - "optical" linear Landweber iteration

small phases \rightarrow linear intensity:

$$Q(\phi) \approx \frac{1}{\epsilon} ml(\epsilon\phi) \quad \text{with} \quad \epsilon \ll 1$$

adjoint:

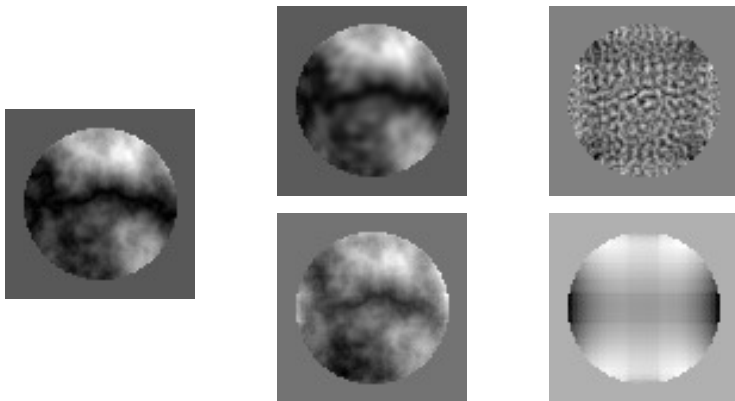
$$Q = Q^*$$

linear iterative Landweber algorithm:

$$\Phi_{k+1} = \Phi_k + \alpha Q^*(ml(\Phi_?) - Q(\Phi_k))$$

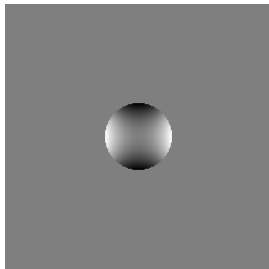
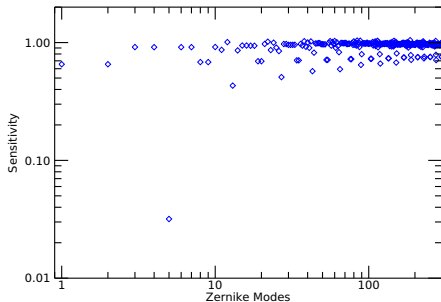
$\Phi_?$ is the phase-to-be-measured/reconstructed, Q the wavefront sensor operator and $ml(\Phi_?)$ the corresponding meta-intensity.

Quad wavefront sensor: first numerical results - “optical” linear Landweber iteration



Left to right: incoming, reconstructed, residual phase.
Top: interaction-matrix-based inversion. Bottom: linear Landweber iteration.

i Quad wavefront sensor: the unseen mode of the i Quad



Sensitivity curve for the i Quad sensor wrt. Zernike modes (left) and the mode (vertical astigmatism) with the low sensitivity (right).

Conclusions

- model-based reconstructors are promising alternatives to MVM approaches
 - no calibration of interaction matrix needed
 - reconstruction qualities are highly comparable (in end2end simulations & on testbed)
- adaptations of existing methods to ELT effects is necessary
- possibilities to combine mathematical theory and optical considerations

Conclusions

- model-based reconstructors are promising alternatives to MVM approaches
 - no calibration of interaction matrix needed
 - reconstruction qualities are highly comparable (in end2end simulations & on testbed)
- adaptations of existing methods to ELT effects is necessary
- possibilities to combine mathematical theory and optical considerations

Outlook:

- derivation of a general framework for reconstructors of Fourier-based wavefront sensors
- comparison of “optical“ reconstruction approaches and model-based implementations

Thank you for your attention

- R. Ragazzoni. *Pupil plane wavefront sensing with an oscillating prism*, J. of Modern Optics 42(2), 289–293, (1996).
- C. Vérinaud. *On the nature of the measurements provided by a pyramid wave-front sensor*, Optics Communication 233, (2004).
M. Rosensteiner. *Wavefront reconstruction for extremely large telescopes via CuRe with domain decomposition*. J. Opt. Soc. Am. A 29.11, 2328-2336 (2011).
Iu. Shatokhina, A. Obereder, R. Rosensteiner, R. Ramlau. *Preprocessed cumulative reconstructor with domain decomposition: a fast wavefront reconstruction method for pyramid wavefront sensor*. Applied Optics 52(12), 2640-2652 (2013).
- V. Hutterer, R. Ramlau. *Non-linear wavefront reconstruction methods for pyramid sensors using Landweber and Landweber-Kaczmarz iteration*. Applied Optics 57(30), 8790–8804, (2018).
- V. Hutterer, Iu. Shatokhina, A. Obereder, R. Ramlau. *Advanced reconstruction methods for segmented ELT pupils using pyramid sensors*. J. Astron. Telesc. Instrum. Syst. 4(4), 049005, (2018).
- V. Hutterer, R. Ramlau, Iu. Shatokhina. *Real-time Adaptive Optics with pyramid wavefront sensors: A theoretical analysis of the pyramid sensor model*, Inverse Problems, <https://doi.org/10.1088/1361-6420/ab0656>.
- V. Hutterer, R. Ramlau, Iu. Shatokhina. *Real-time Adaptive Optics with pyramid wavefront sensors: Accurate wavefront reconstruction using iterative methods*, Inverse Problems, <https://doi.org/10.1088/1361-6420/ab0900>.